Dynamics of Proteins in Hydrated State and in Solution As Studied by Dielectric Relaxation Spectroscopy

Jovan Mijović,* Yu Bian, Richard A. Gross, and Bo Chen

Othmer Department of Chemical and Biological Sciences and Engineering, Polytechnic University, Six Metrotech Center, Brooklyn, New York 11201

Received August 23, 2005; Revised Manuscript Received October 11, 2005

ABSTRACT: An investigation was carried out of the interactions between water and three globular proteins: Candida antarctica Lipase B (CaLB), Bovine Serum Albumin (BSA), and Lysozyme (Lys). Measurements were performed on hydrated proteins and protein solutions using dielectric relaxation spectroscopy over a wide range of frequency (10^{-2}−10^{9} Hz) and temperature (−100 to +80 °C). Three dielectric dispersions were observed in hydrated proteins, and an explanation of their molecular origin was offered in terms of the three regions in globular proteins where the absorbed water is located. Those three processes evolve gradually into an overlapping broad dispersion with increasing water content and temperature; this finding was common to hydrated proteins and aqueous solutions alike. Dielectric modulus formalism was employed to compare the dynamics of proteins in aqueous and nonaqueous solutions in the temperature range from 20 to 80 °C. Dimethyl sulfoxide (DMSO) was the nonaqueous solvent of choice because of its ability to interfere with hydrogen bonding. General trends in aqueous and nonaqueous solutions are similar but with notably different time scales. For a given concentration and temperature, the relaxation process is slower in DMSO than in the aqueous solution. Low-temperature (below 0 °C) dynamics in aqueous solutions were characterized by the presence of two processes: their origin and their temperature and concentration dependence are discussed.

Introduction

Protein−water interactions are known to influence the structure and the function of proteins.[1−5] The studies of protein−water interactions could be classified into two groups:[6,7] (1) hydrated proteins, where water is absorbed on the surface of the protein powder and the water level does not exceed the critical hydration required to cover the protein molecules with up to two layers of water, and (2) protein solutions. Early studies of protein−water interactions by dielectric measurements were conducted over a narrow range of frequency and temperature and were reviewed in 1992 by Pethig.[6] Several relaxation processes were claimed and attributed to motions that range from the side groups in proteins to the various layers of strongly and/or weakly bound water. But the interpretation of data and the identification of the molecular origin of the observed processes have been difficult due to the narrow range of frequency and temperature used and the limitations of the early instrumentation.

In 1996, Bone[8] reported room temperature measurements of hydrated lysozyme in the frequency range from 100 kHz to 10 GHz using time domain reflectometry (TDR). He observed two dielectric dispersions in the hydrated lysozyme and assigned them to two layers of adsorbed water. The processes at 10 MHz and 1 GHz are attributed to the first and the seconds layer of adsorbed water, respectively. Careri and co-workers[9−14] studied proton migration in globular proteins. They observed a dielectric dispersion in the kilohertz to megahertz range at room temperature and assigned it to the protons that migrate within the globular protein and are located in ionized side chains, bound water, and nearby backbone peptides. By increasing the water coverage of the protein powder, the bound water clusters exhibit a percolative transition.

Mashimo and co-workers[15−20] published a series of reports on the measurements of dielectric properties of aqueous solution of globular proteins by TDR in the frequency range from 100 kHz to 10 GHz. Three kinds of water were identified: bulk water, which freezes at −5 °C, unfreezable water, which constructs a shell layer around the protein molecule, and bound water, which attaches directly to the protein surface. A salt reference, adjusted to have the same dc conductivity as the protein solution, was used to diminish the effect of conductivity. Bonincontro and co-workers[7,21−27] investigated aqueous solutions of proteins by DRS in the frequency range from 100 kHz to 1 GHz. A dielectric dispersion was observed in the megahertz range and attributed to the protein structure. They also obtained an estimate of the average molecular radius and the dipole moment.

In general, protein−water interactions are not fully understood, and most of the work was done in either aqueous solution or the hydrated state.[3−31] The aim of the present work was to gain a deeper insight into the nature of protein−water dynamics by conducting an investigation of the same proteins in the hydrated state and in solution. Three different globular proteins were examined, and novel information is generated and presented through the use of wide temperature and frequency range in DRS measurement.

Experimental Section

Materials. The three proteins investigated, Candida antarctica Lipase B (CaLB), Bovine Serum Albumine (BSA), and Lysozyme (Lys), are described in Table 1. CaLB was obtained from Novo Nordisk, BSA, from Sigma and Lys from Boehringer Mannheim. All proteins were dialyzed three times.

Protein solutions were made in deionized water. Hydrated proteins were obtained in a closed humidifier by exposing the protein powder to water vapor at a desired relative humidity.

* To whom correspondence should be addressed. E-mail: jmijovic@poly.edu.

10.1021/ma051854c CCC: $30.25
Published on Web 11/12/2005

Table 1. Proteins Investigated

protein composition	Lys	CaLB	BSA
mol wt [Da]	18626	33008	67000
no. of residues	164	317	583

Table 2. Water Content of Hydrated Proteins at Different Humidity

humidity	0	0.1	0.45	0.75
water content (wt %)	10	15	22	27

Vacuum and salt solutions were used to control the humidity. Water content of hydrated proteins at different humidity was measured and is summarized in Table 2.

The activity of proteins was assayed by hydrolysis.[32−35] The change in the absorption rate of the reactant was monitored by a UV−vis spectrophotometer (Spectra Max plus 384, Sunnyvale, CA). The denatured protein lost more than 90% of the activity in the native state.

Techniques. *Dielectric Relaxation Spectroscopy (DRS).* Our facility combines commercial and custom-made instruments that include (1) Novocontrol α high-resolution dielectric analyzer (3 μHz−10 MHz) and (2) Hewlett-Packard 4291B rf impedance analyzer (1 MHz−1.8 GHz). Both instruments are interfaced to computers and equipped with heating/cooling controls, including the Novocool system custom-modified for measurements over the entire frequency range from 3 μHz to 1.8 GHz. The protein samples were placed between the stainless steel electrodes (identical results were obtained with aluminum electrodes) and surrounded by a Teflon ring. The diameter of the electrodes is 10 mm, and the thickness of the samples is measured before each measurement (typical thickness was about 200 μm). Further details of our DRS facility are given elsewhere.[36,37]

Differential Scanning Calorimetry (DSC). A TA Instruments Co. DSC model 2920 was used. The proteins were placed in sealed DSC pans and scanned at a heating or cooling rate of 5 °C/min.

Results and Discussion

We preface the discussion of our results by pointing out that the fundamental aspects of DRS, theoretical and experimental, are well established and will not be discussed here; the interested reader is referred to a number of excellent books and key reviews.[38−40] The presentation of the results is subdivided into two parts: (1) dynamics of hydrated proteins and (2) dynamics of protein solutions.

1. Dynamics of Hydrated Proteins. We begin by examining the dielectric response of hydrated proteins. Dielectric loss in the frequency domain for CaLB, BSA, and Lys, measured at −60 °C, is shown in Figure 1, and the ionic contribution was not subtracted. The water content in each protein was 15 wt %. The three processes observed in the frequency window of Figure 1 are termed α, β, and γ in the order of increasing frequency at constant temperature. We note, however, that the Greek letters are used for convenience, and the observed processes should not be identified with the well-documented segmental (α) and local (β, γ) relaxations in glass-forming materials.[41,42] It is also interesting to note that changes in temperature or water content have analogous effect on the dielectric response of the three proteins investigated in this study. Consequently, in the text below we shall frequently present the results for only one protein, with an understanding that those results exemplify a general trend.

We next consider the effect of temperature on the dielectric response in more detail using CaLB as the representative protein. Dielectric loss of CaLB in the frequency domain at a constant water content and with

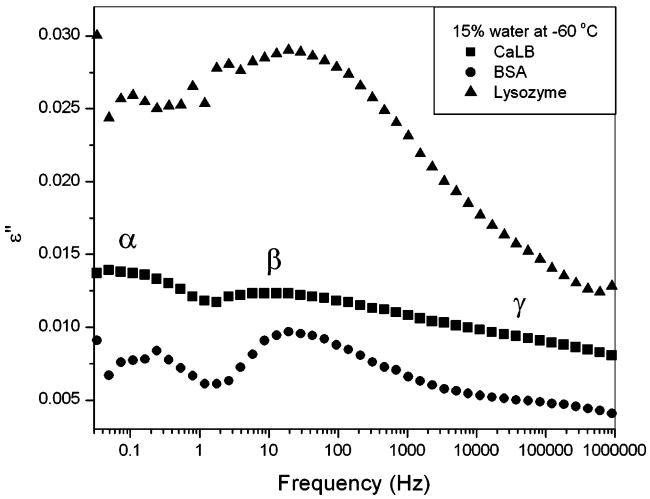

Figure 1. Dielectric loss of CaLB, Lys, and BSA in the frequency domain. The water content in all proteins was 15%, and the spectra were obtained at −60 °C.

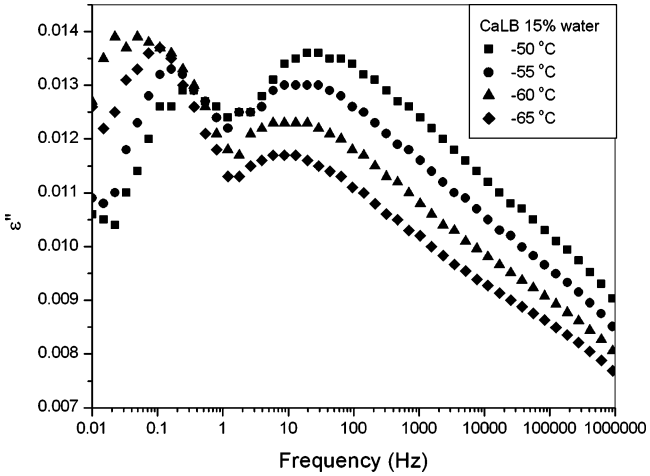

Figure 2. Dielectric loss of CaLB in the frequency domain at different temperature. The water content was constant at 15%.

temperature as a parameter is shown in Figure 2. Two principal observations are made. First, the α process shifts to higher frequency and decreases in intensity with increasing temperature. And second, the broad transition that encompasses the β and γ processes also shifts to higher frequency but increases in intensity with increasing temperature.

The effect of varying water content on the dielectric response is considered next. Figure 3 illustrates real permittivity and loss of hydrated BSA in the frequency domain, measured at −60 °C, with water content (between 10 and 27%) as a parameter. Both loss and real permittivity increase with increasing water content. The three processes that characterize the dielectric loss spectra of hydrated proteins, α, β, and γ (Figure 1) are readily distinguishable at low water content. However, with increasing water content, those three processes evolve gradually into a broad spectrum at which point a physically meaningful separation of the overlapping processes is not possible. At the water content of 27%, for example, the low-frequency end of the spectrum is dominated by conductivity and electrode polarization, masking the α process completely.

Whenever it was physically meaningful (i.e., at lower water content), the experimentally obtained spectra were deconvoluted using the well-known Havriliak−

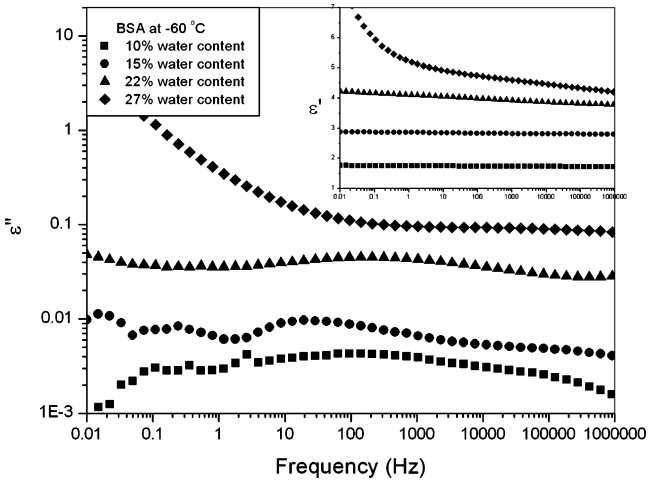

Figure 3. Dielectric permittivity (inset) and loss of BSA in the frequency domain with variable water content. Spectra were obtained at −60 °C.

Negami (HN) functional form:[43]

$$\epsilon^*(\omega) = \epsilon_\infty + \frac{\epsilon_0 - \epsilon_\infty}{[1 + (i\omega\tau_{HN})^a]^b} \quad (1)$$

where a and b are the spectral shape parameters, and τ_{HN} is the average relaxation time obtained from the fits. Note that the HN function reduces to the Cole−Davidson equation[44] for $a = 1$ and the Cole−Cole equation[45] for $b = 1$.

Deconvolution of a CaLB spectrum into three individual processes, illustrated in Figure 4, was accomplished using three HN functions and a conductivity term ($\sigma/(\omega\epsilon_v)$, where σ is the conductivity and ϵ_v is the vacuum permittivity. The best-fit HN parameters for each process are listed in Table 3. We note that the HN parameters a and b measure the breadth and the symmetry of the spectrum, respectively. The α process is Debye-like ($a = b = 1$) and thermally activated, with an activation energy of 14.27 kJ/mol calculated using the Arrhenius form of the temperature dependence of the average relaxation time for the α process. This activation energy is slightly lower than the average activation energy for the hydrogen bond. The β process is asymmetric, and it broadens with increasing temperature; the HN shape parameter "a" decreases from 0.5 to 0.36 for CaLB and Lys and from 0.8 to 0.6 for BSA. Interestingly, broadening takes place largely over a temperature range from 210 to 240 K for CaLB and Lys and from 230 to 260 K for BSA. DSC measurements were run in search of a physical transition in that temperature range that could be interpreted as the underlying cause for the observed broadening, but none was found. Nevertheless, we acknowledge reports in the literature[46−48] of the existence of "glass transition" ("T_g") in hydrated proteins that decreases with increasing hydration. It is curious to note that the temperature range in which the HN shape parameter a changes corresponds to the reported range for "T_g" in Lys. The implication would be that the dynamics of bound water are affected by the "T_g" of the protein. Finally, the γ process is symmetric, but it broadens slightly (a decreases from 0.4 to 0.3) with increasing temperature.

The temperature dependence of the average relaxation time for each process (obtained from the HN fits) was determined, and the results are plotted in Figure 5 (the β' process seen in the aqueous solutions of CaLB, also included in Figure 5, will be discussed in the protein solution part). Several interesting observations are made. There is no indication of the Vogel−Fulcher−Tammann (VFT) behavior; notwithstanding some data scatter, the temperature dependence of the average relaxation time for each process is of the Arrhenius type. It is also interesting that the activation energy varies from one process to another (see Table 3) but is not a function of the type of protein.

The results presented thus far were obtained on proteins in their native state and it was of interest to investigate the dielectric response of denatured proteins.[32−35,49,50] Denaturation was accomplished by heating for 24 h at 120 °C and then exposing the proteins to 10% relative humidity to reabsorb water. Dielectric loss in the frequency domain for the denatured CaLB with temperature as a variable is shown in Figure 6a. The three characteristic processes described earlier, α, β, and γ, are again observed; however, their strengths are lower than in the native protein, and the data for the α process are scattered. The broad transition that encompasses β and γ processes shows a systematic shift to higher frequency with increasing temperature. A direct comparison of the dielectric response of native and denatured CaLB with 15% water content, measured at −60 °C, is shown in Figure 6b. The strength and the shape of β and γ processes in native and denatured states are similar, but the strength of the α process decreases noticeably after denaturation. Analogous trends were observed in the denatured BSA and Lys, but those results are not shown here.

The water content in hydrated proteins typically varies between 10 and 25 wt %, and the calculations show that a monolayer coverage is attained at about 25 wt %.[6] The picture of water−protein interactions in hydrated proteins, which emerges from our DRS study, is as follows. There are three regions where water binds to the protein surface, as illustrated in Figure 7. We term those regions I, II, and III and examine their origin. Region I is associated with the α process. Because the α process is not fully recovered upon denaturation, it is likely that it involves water−protein interactions in the regions that undergo major structural change during denaturation. The long time scale (low frequency) and the low activation energy (see Table 3) suggest that the molecular and collective dynamics of water−protein interactions are determined by the counterbalance of surface and confinement effects in the inner potion of the protein.[51] The motion of bound water that partakes in the α process is impeded by the surrounding protein (confinement effect), but its activation energy is not affected (surface effect). Thus, the overall dipole moment remains unchanged, and the $\Delta\epsilon$ of the α process decreases with increasing temperature. Region II is associated with the β process. Higher activation energy suggests stronger water−protein interactions. One interesting observation regards the so-called "T_g", reported in the literature but not detected in our DSC measurements. As stated earlier, the β process undergoes a noticeable change in the "T_g" range for all proteins, manifest in the spectral broadening with increasing temperature. Region III is associated with the shortest time scale and length scale process, i.e., the γ process. Extrapolation of the γ process to 25 °C yields the value of relaxation time (10^{-8} s) similar to that of the first layer bound water measured by Bone.[8] This suggests that the origin of the γ process lies in the water molecules that attach loosely to the protein surface.

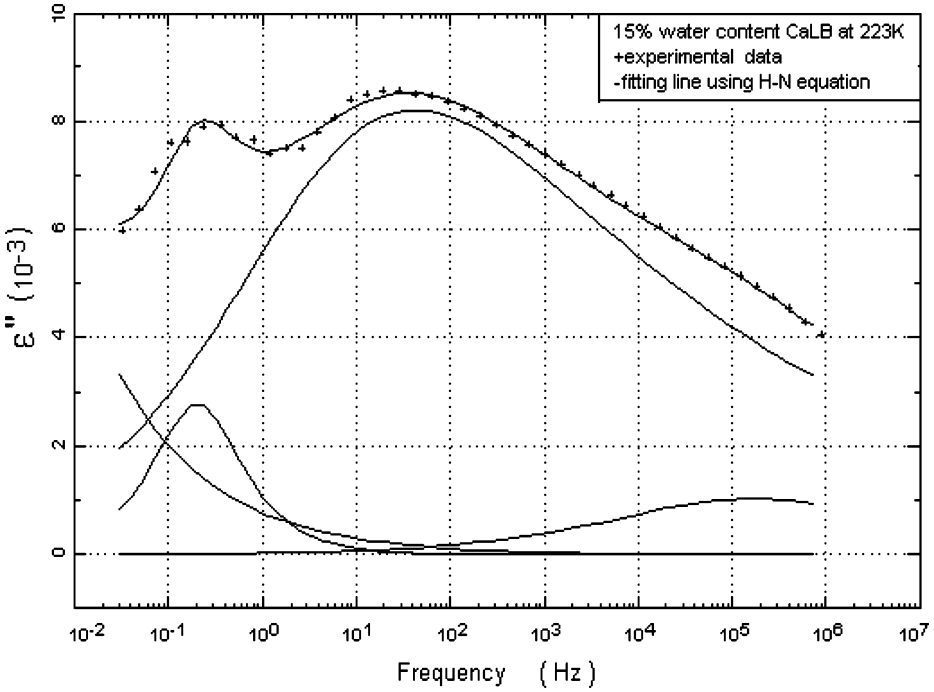

Figure 4. Deconvolution of a dielectric loss spectrum of CaLB with 15% water content, measured at 223 K. Solid lines are fits to the HN functional form.

Table 3. Activation Energies and Best-Fit HN Parameters for the α, *β*, and *γ* Processes in Hydrated CaLB, Lys, and BSA

	α	*β*		*γ*
activation energy (kJ/mol)	14	36		19
a	1.00	0.5−0.36 for CaLB and Lys	0.8−0.6 for BSA	0.4−0.3
b	1.00	0.3		1.0

2. Dynamics of Proteins in Solution. a. High-Frequency, High-Temperature Dynamics. We next turn our attention to the dynamics of proteins in aqueous and nonaqueous solutions over a wide range of frequency and temperature. Dimethyl sulfoxide (DMSO) was the nonaqueous solvent of choice because of its ability to interfere with hydrogen bonding. High-frequency behavior is addressed first. At room temperature, conductivity is lower in the DMSO than in the aqueous solutions, but it is still sufficiently high to mask any relaxation processes well into the megahertz range, as illustrated in Figure 8. Dielectric spectra are generally represented using the permittivity formalism, but in highly charged materials, such as DNAs and ionic glasses or melts, dielectric modulus is the preferred form of data representation.[52] Dielectric modulus is the reciprocal of the complex permittivity and is given as

$$M^*(\omega) = \frac{1}{\epsilon^*} = M'(\omega) + iM''(\omega) \qquad (2)$$

Dielectric loss modulus in the frequency domain for 1 mg/mL aqueous solution of CaLB in the temperature range between 10 and 50 °C is shown in Figure 9a. The

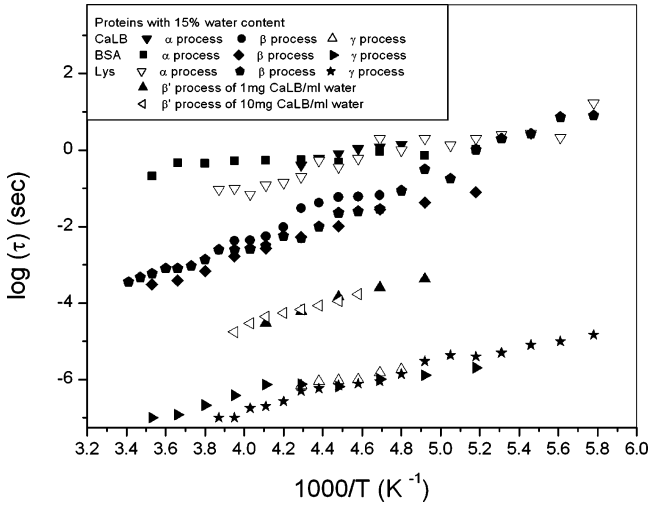

Figure 5. Average relaxation time for the α, *β*, and *γ* processes in hydrated proteins with 15% water content as a function of reciprocal temperature.

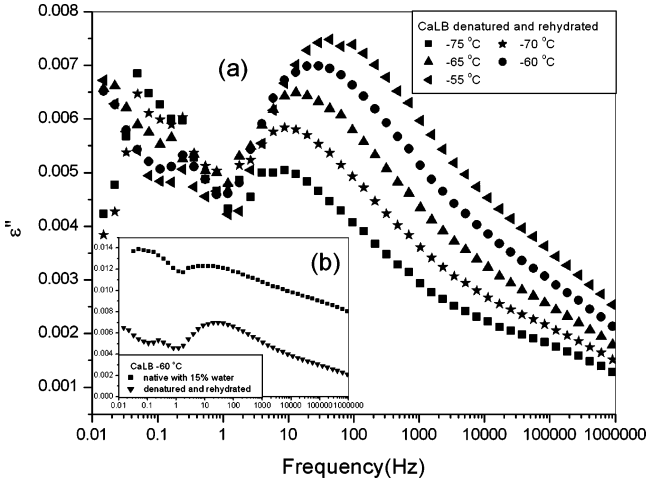

Figure 6. (a) Dielectric loss of denatured CaLB in the frequency domain at different temperature. (b) Dielectric loss of native and denatured CaLB in the frequency domain. Water content was 15%, and the spectra were obtained at −60 °C.

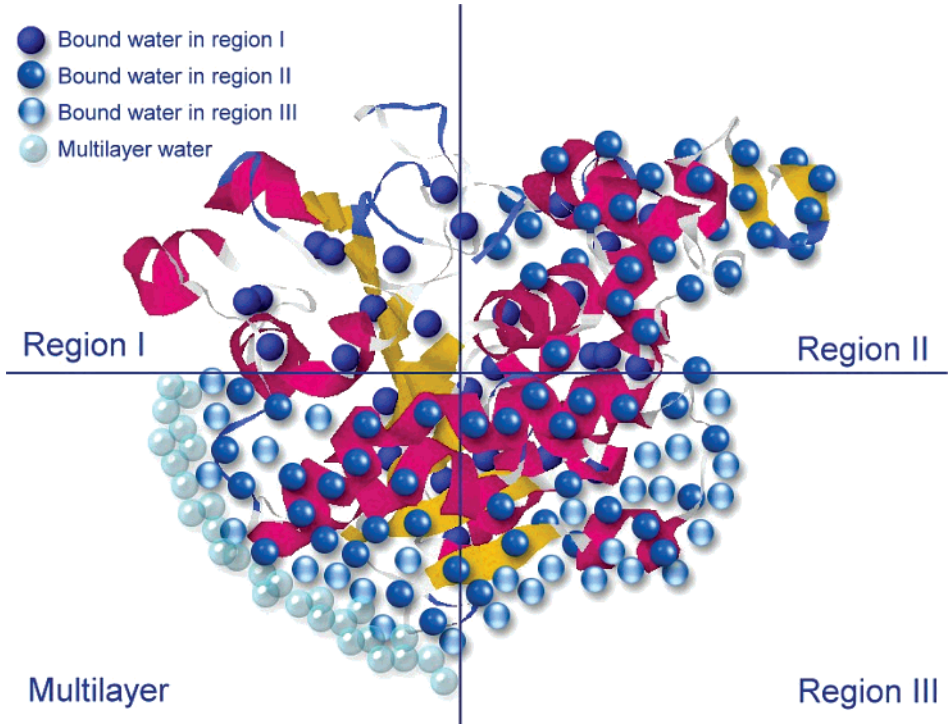

Figure 7. Schematic illustration of the three regions where binds to the protein.

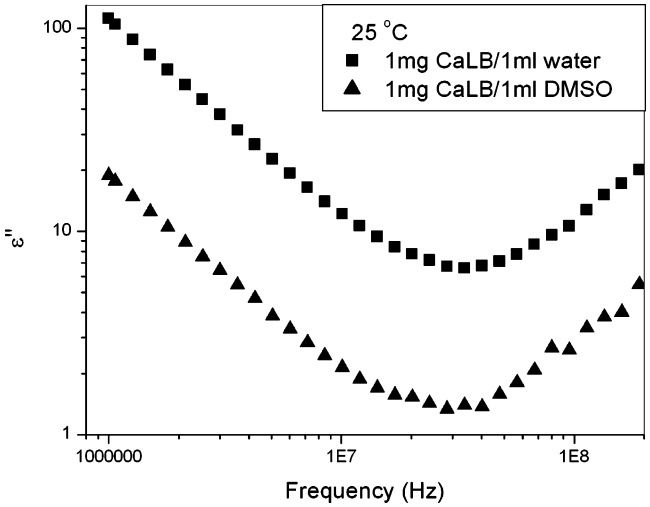

Figure 8. Dielectric loss of 1 mg/mL CaLB solution in the frequency domain at 25 °C. Solid symbols, aqueous solution; open symbols, DMSO solution.

loss modulus peak shifts to higher frequency and increases in intensity with increasing temperature. The characteristic time, calculated as the inverse of the angular frequency at maximum loss modulus, is often referred to as conductivity relaxation time. A 10-fold increase in CaLB concentration affects the spectrum as illustrated in Figure 9b, which depicts the loss modulus spectrum of a 10 mg/mL aqueous solution in the temperature range between 10 and 50 °C. There is a noticeable shift in the loss modulus peak to higher frequency with increasing temperature. It is interesting that for any given temperature the conductivity relaxation time decreases (higher frequency, faster process) with increasing CaLB concentration. That is readily seen by comparing parts a and b of Figure 9.

Dielectric modulus spectra of the DMSO solutions of CaLB were obtained in the temperature range between 20 and 80 °C. Data for 1 and 10 mg/mL DMSO solutions

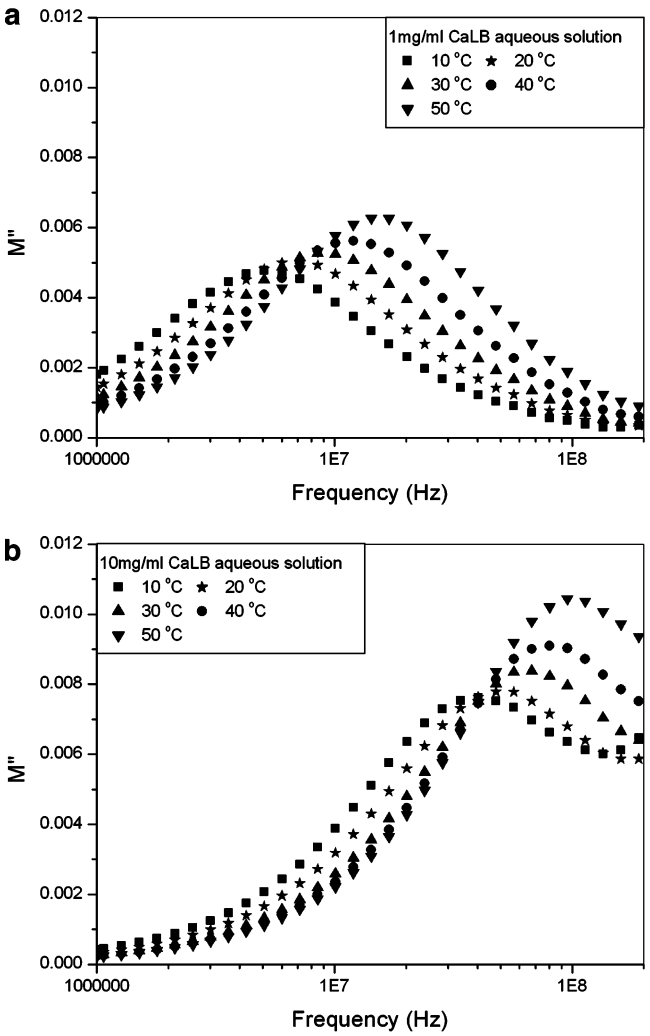

Figure 9. Dielectric loss modulus of the aqueous solution of CaLB in the frequency domain with temperature as a parameter: (a) 1 mg/mL; (b) 10 mg/mL.

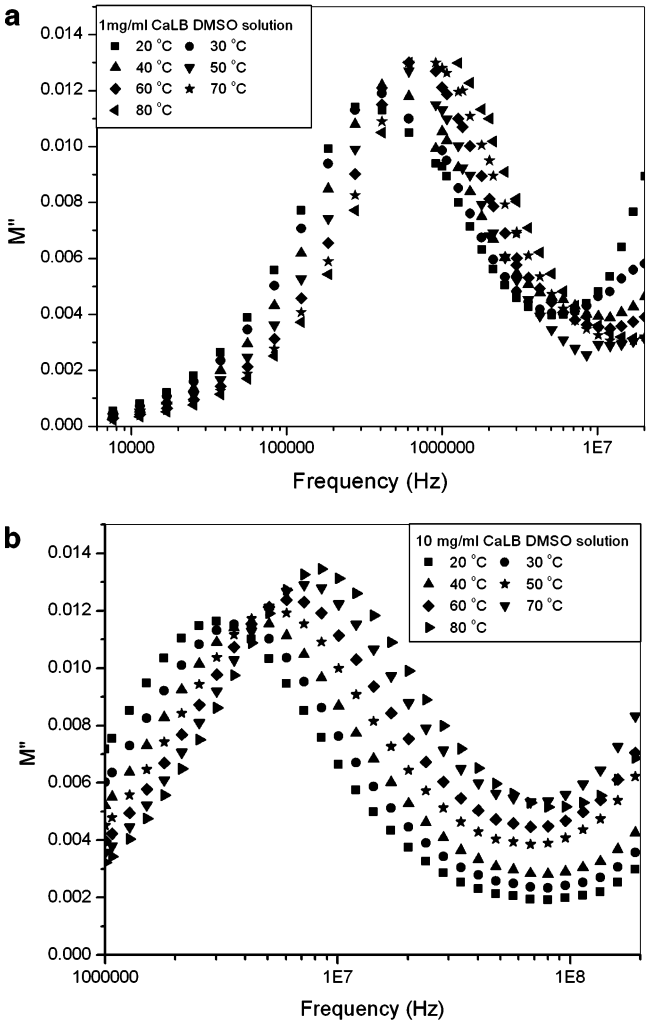

Figure 10. (a) Dielectric loss modulus of the DMSO solution of CaLB in the frequency domain with temperature as a parameter: (a) 1 mg/mL; (b) 10 mg/mL.

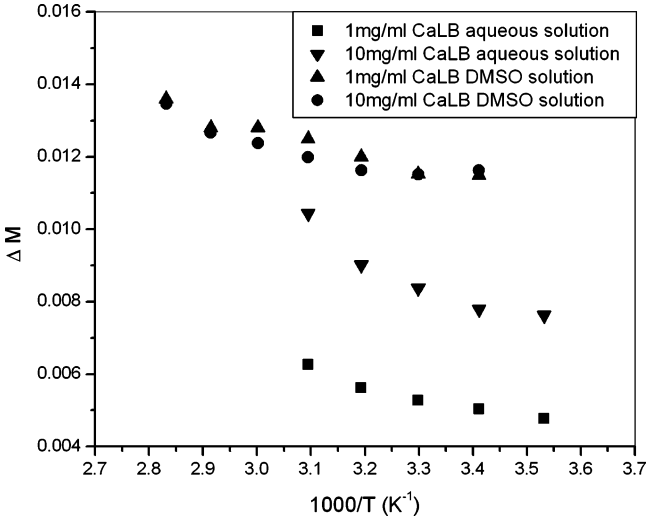

Figure 11. Dielectric modulus strength for aqueous and DMSO solutions of CaLB as a function of reciprocal temperature with concentration as a parameter.

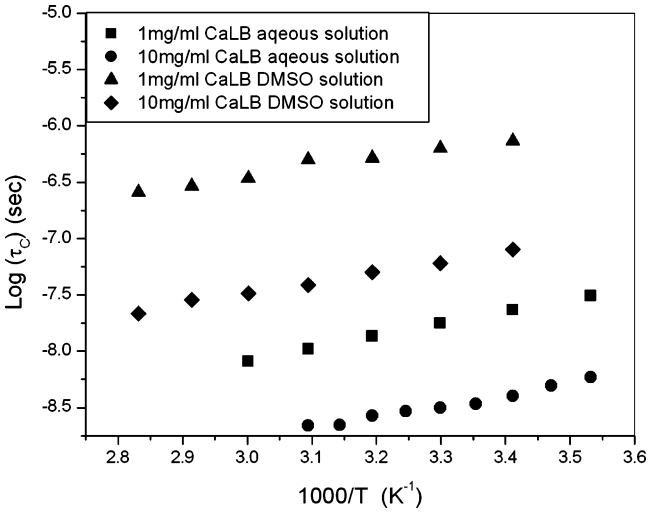

Figure 12. Conductivity relaxation time for aqueous and DMSO solutions of CaLB as a function of reciprocal temperature with concentration as a parameter.

of CaLB are shown in parts a and b of Figure 10, respectively. General trends are similar to those observed in the aqueous solutions but with notably different time scales. For a given concentration and temperature, the relaxation process is considerably slower in DMSO than in the aqueous solution. This is evident by comparing Figures 9a and 10a and Figures 9b and 10b. The dielectric modulus strength (ΔM) of both aqueous and DMSO solution increases with increasing temperature, as shown in Figure 11. Three principal findings are (1) ΔM is lower in the aqueous than in the DMSO solution at the same protein concentration and temperature, (2) ΔM is not a function of protein concentration in the DMSO solution but it increases with increasing concentration in the aqueous solution, and (3) the temperature dependence of the conductivity relaxation time for CaLB solutions shown in Figure 12 is of the Arrhenius type with an activation energy of 19 kJ/mol, independent of the type of solvent and protein concentration. The shorter conductivity relaxation time in the aqueous solutions and higher protein concentration is in accordance with the Barton/Nakajima/Namikawa[53,54] (BNN) relationship.

In sum, a comparison of the dielectric spectra of aqueous and DMSO solutions reveals that the dynamics of proteins are dominated by the solvent. We note that Caliskan et al.[55] have reached the same conclusion in their study of proteins in different solvents and that the analogous result was obtained in aqueous and nonaqueous solutions of DNA.[56]

b. Low-Temperature Dynamics. Extensive measurements were performed on all three proteins at temperatures below 273 K. Dielectric loss and real permittivity in the frequency domain for 1 and 10 mg/mL aqueous solutions of Lys are shown in Figures 13 and 14, respectively. There is an increase in both real

Table 4. Activation Energies and Best-Fit HN Parameters for the α′ and β′ Processes in Aqueous Solutions of CaLB, Lys, and BSA; Results for Ice Are Included for Comparison

	α′ of Lys	α′ of BSA	β′ of Lys	β′ of BSA	β′ of CaLB	ice
activation energy (kJ/mol) for 1 mg/mL	44	47	24	27	26	48
activation energy (kJ/mol) for 10 mg/mL	43	43	24	24	25	
a	0.95		0.80			0.95
b	1.00		1.00			1.00

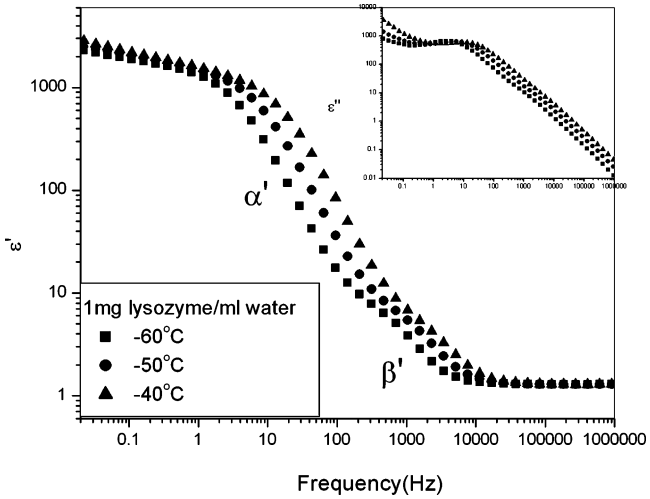

Figure 13. Dielectric loss (inset) and real permittivity of 1 mg/mL aqueous solution of Lys in the frequency domain with temperature as a parameter.

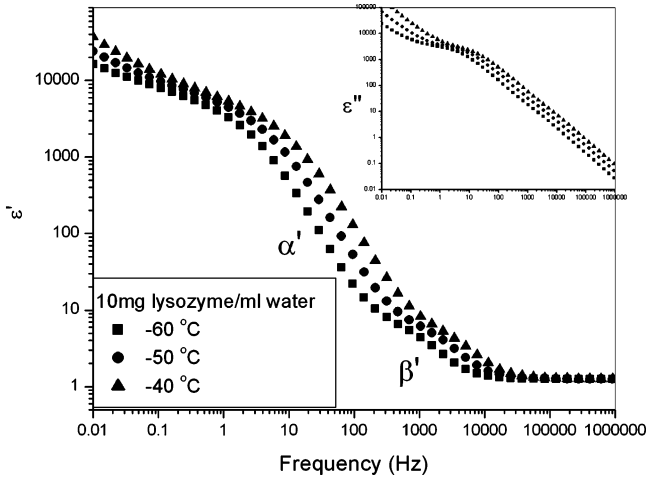

Figure 14. Dielectric loss (inset) and real permittivity of 10 mg/mL aqueous solution of Lys in the frequency domain with temperature as a parameter.

permittivity and loss with increasing protein concentration. Dielectric loss is quite high and the spectra are broad, but the two-step change in real permittivity is a clear signature of the presence of two processes.

The two processes observed in the frequency window of Figures 13 and 14 are termed α′ and β' in the order of increasing frequency at constant temperature. Deconvolution of the measured dielectric response into two HN terms was carried out, and the best-fit HN parameters are listed in Table 4. Both processes are symmetric, but the β' process is slightly broader. The responses of Lys, BSA, and CaLB are very similar; an exception is the α′ process of CaLB which is largely masked by conductivity, precluding physically meaningful fits to the HN equation.

The temperature dependence of the average relaxation time for each process (obtained from the HN fits) is plotted in Figure 15, and the activation energies are listed in Table 4. The α′ process has an activation energy of 50 kJ/mol, the same as that of pure ice. Below approximately −50 °C the relaxation time increases more slowly with decreasing temperature, showing an activation energy of 20 kJ/mol. We note that pure deionized water follows the same trend as the protein solutions within the same temperature range.[57] This

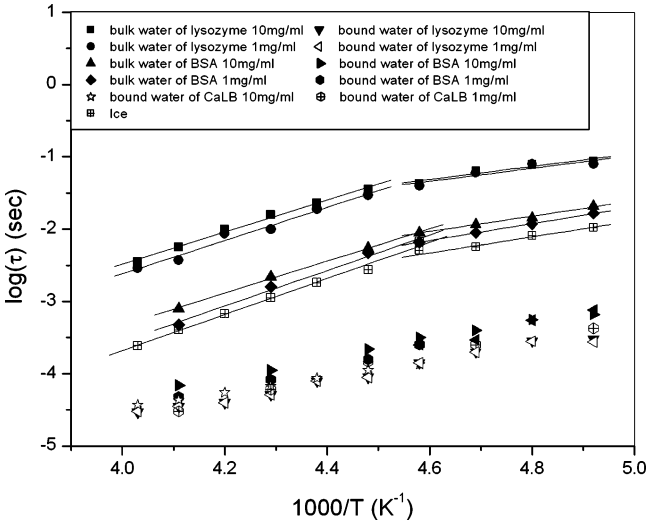

Figure 15. Average relaxation time for the α′ and β' processes in aqueous solutions of different proteins at different concentrations as a function of reciprocal temperature. Solid lines are fits to the Arrhenius equation.

further supports the tenet that the α′ process originates from ice in the protein−ice matrix.

Interestingly, the activation energy of the β' process does not vary with the type or the concentration of protein and is approximately constant at 25 kJ/mol. The relaxation time and the activation energy of the β' process lie between those for the β and γ processes in hydrated proteins shown in Figure 5. This suggests that the β' process represents a combination of different bound water processes. The implication is that there is a correspondence between the bound water in hydrated proteins and in protein solutions.

Conclusions

We have completed an investigation of the dynamics of three globular proteins, CaLB, BSA, and Lys, in the hydrated state and in solution. This work has added new information to the past efforts aimed at understanding the protein−water interactions. Dynamics were measured by dielectric relaxation spectroscopy over the frequency range from 10^{-2} to 10^{9} Hz and at temperature from −100 to +80 °C.

Three dielectric processes are observed in hydrated proteins and are believed to originate in the interactions between the protein and the first layer of bound water. With increasing water content and temperature, however, those three processes overlap and evolve into a single broad dispersion. Each process is Arrhenius-like and is not a function of the type of protein. The low-frequency α process originates in the inner portion of the protein and cannot be fully recovered upon denaturation because it involves water−protein interactions at sites that undergo major functional or structural change. The other two processes, β and γ, are reversible upon denaturation. The HN parameter "a" of the β process undergoes a noticeable decrease in the "T_g" range for all proteins, but the underlying physics is not clear. The γ process is characterized by the shortest time scale and length scale. Extrapolation of the γ process to 25 °C yields the value of relaxation time (10^{-8} s) similar to that for the first layer bound water measured by Bone.[8] This suggests that the origin of the γ process lies in the water molecules that attach loosely to the protein surface.

Both aqueous and DMSO protein solutions in the temperature range from 20 to 80 °C are characterized by a pronounced dielectric loss modulus peak that shifts to higher frequency with increasing temperature and protein concentration. But for the same protein concentration, this process is slower in DMSO than in the aqueous solution. The temperature dependence of the conductivity relaxation time for all protein solutions is of the Arrhenius type with the activation energy of 19 kJ/mol. Low-temperature measurements reveal two processes, termed α' and β' in the order of increasing frequency at constant temperature. The α' process originates from ice in the protein−ice matrix, and this is supported by the fact that pure deionized water shows the same trend as the protein solutions within the same temperature range. The relaxation time and the activation energy of the β' process lie between those for the β and γ processes in hydrated proteins, suggesting that the β' process represents an average combination of different bound water processes.

In sum, the combined dielectric study of hydrated proteins and protein solutions affords the following overall view of water−protein interactions. The picture that emerges is suggestive of the presence of three regions, or binding sites, on globular proteins where the first layer of water binds. An interpretation of the molecular origin of the ensuing water−protein interactions is as follows.

(1) Region I encompasses binding sites within the inner portion of the protein. Bound water in this region engages the key functional sites in the 3D structure of the protein, and those interactions are largely irreversible upon denaturation.

(2) Region II includes binding sites on the polypeptide backbone and the polar groups. This region accounts for the main portion of the first layer of bound water, and it appears to be sensitive to the so-called "T_g" of the protein. The water−protein interactions in this region are reversible upon denaturation.

(3) Region III is represented by the weakly bound water, and some multilayer formation is possible. Bound water in this region is also reversible upon denaturation.

Acknowledgment. This material is based, in part, on work supported by National Science Foundation under Grant DMR-0101182.

References and Notes

(1) Lindorff-Larsen, K.; Best, R. B.; Depristo, M. A.; Dobson, C. M.; Vendruscolo, M. *Nature (London)* **2005**, *433*, 128.
(2) Benkovic, S. J.; Hammes-Schiffer, H. *Science* **2003**, *301*, 1196.
(3) Otting, G.; Wuthrich, K. *J. Am. Chem. Soc.* **1989**, *111*, 1871.
(4) Baker, E. N.; Hubbard, R. E. *Prog. Biophys. Mol. Biol.* **1984**, *44*, 97.
(5) Saenger, W. *Annu. Rev. Biophys. Biophys. Chem.* **1987**, *16*, 93.
(6) Pethig, R. *Annu. Rev. Phys. Chem.* **1992**, *43*, 177.
(7) Bonincontro, A.; Risuleo, G. *Spectrochim. Acta, Part A* **2003**, *59*, 2677.
(8) Bone, S. *Phys. Med. Biol.* **1996**, *41*, 1265.
(9) Levstik, A.; Filipic, C.; Kutnjak, Z.; Careri, G.; Consolini, G. *Phys. Rev. E* **1999**, *60*, 7604.
(10) Bruni, F.; Careri, G.; Leopold, A. C. *Phys. Rev. A* **1989**, *40*, 2903.
(11) Careri, G.; Giansanti, A.; Rupley, J. A. *Proc. Natl. Acad. Sci. U.S.A.* **1986**, *83*, 6810.
(12) Careri, G.; Consolini, G.; Bruni, F. *Solid State Ionics* **1999**, *125*, 257.
(13) Careri, G.; Milotti, E. *Phys. Rev. E* **2003**, *67*, 051923.
(14) Pizzitutti, F.; Bruni, F. *Phys. Rev. E* **2001**, *64*, 052905.
(15) Miura, N.; Hayashi, Y.; Shinyashiki, N.; Mashimo, S. *Biopolymers* **1995**, *36*, 9.
(16) Mashimo, S.; Umehara, T.; Ota, T. *J. Mol. Liq.* **1987**, *36*, 135.
(17) Hayashi, Y.; Shinyashiki, N.; Yagihara, S. *J. Non-Cryst. Sol.* **2002**, *305*, 328.
(18) Miura, N.; Asaka, N.; Shinyashiki, N.; Mashimo, S. *Biopolymers* **1994**, *34*, 357.
(19) Mashimo, S.; Miura, N.; Shinyashiki, N.; Ota, T. *Macromolecules* **1993**, *26*, 6859.
(20) Mashimo, S.; Miura, N. J. *Chem. Phys.* **1993**, *99*, 9874.
(21) Bonincontro, A.; Mari, C.; Mengoni, M.; Risuleo, G. *Biophys. Chem.* **1997**, *67*, 43.
(22) Bonincontro, A.; Cinelli, S.; Onori, G.; Stravato, A. *Biophys. J.* **2004**, *86*, 1118.
(23) Bonincontro, A.; Bultrini, E.; Calandrini, V.; Onori, G. *Phys. Chem. Chem. Phys.* **2001**, *3*, 3811.
(24) Bonincontro, A.; De Francesco, A.; Onori, G. *Colloids Surf. B: Biointerfaces* **1998**, *12*, 1.
(25) Bonincontro, A.; De Francesco, A.; Onori, G. *Chem. Phys. Lett.* **1999**, *301*, 189.
(26) Bonincontro, A.; Calandrini, V.; Onori, G. *Colloids Surf. B: Biointerfaces* **2001**, *21*, 311.
(27) Bonincontro, A.; De Francesco, A.; Matzeu, M.; Onori, G.; Santucci, A. *Colloids Surf. B: Biointerfaces* **1997**, *10*, 105.
(28) Rupley, J. A.; Careri, G. *Adv. Protein Chem.* **1992**, *41*, 37.
(29) Harvey, S. C.; Hoekstra, P. *J. Phys. Chem.* **1972**, *76*, 2987.
(30) Careri, G. *Prog. Biophys. Mol. Biol.* **1998**, *70*, 223.
(31) Grant, E. H.; Sheppard, R. J.; South, G. P. *Dielectric Behaviour of Biological Molecules in Solution*; Clarendon Press: Oxford, 1978.
(32) Giancola, C.; Sena, C. D.; Fessas, D. *Int. J. Biol. Macromol.* **1997**, *20*, 193.
(33) Barone, G.; Giancola, C.; Verdoliva, A. *Thermochim. Acta* **1992**, *199*, 197.
(34) Braianti, A.; Fisicaro, E. *Thermochim. Acta* **1994**, *241*, 131.
(35) Elkordy, A. A.; Forbes, R. T.; Barry, B. W. *Int. J. Pharm.* **2004**, *278*, 209.
(36) Fitz, B.; Andjelic, S.; Mijovic, J. *Macromolecules* **1997**, *30*, 5227.
(37) Mijovic, J.; Miura, N.; Monetta, T.; Duan, Y. *Polym. News* **2001**, *26*, 251.
(38) Williams, G. Dielectric relaxation spectroscopy of amorphous polymer systems: the modern approaches. In *Keynote Lectures in Selected Topics of Polymer Science*; Riande, E., Ed.; CSIC: Madrid, 1997.
(39) Williams, G. Theory of dielectric properties. *In Dielectric Spectroscopy of Polymeric Materials*; Runt, J. P., Fitzgerald, J. J., Eds.; American Chemical Society: Washington, DC, 1997.
(40) Kremer, F., Schonhals, A., Eds.; *Broadband Dielectric Spectroscopy*; Springer-Verlag: Berlin, 2002.
(41) Paluch, M.; Roland, C. M.; Gapinski, J.; Patkowski, A. J. *J. Chem. Phys.* **2003**, *118*, 3177.
(42) Casalini, R.; Livi, A.; Rolla, P.; Levita, G.; Fioretto, D. *Phys. Rev. B* **1996**, *53*, 564.
(43) Havriliak, S. J.; Negami, S. *Polymer* **1967**, *8*, 161.
(44) Davidson, D. W.; Cole, R. H. *J. Chem. Phys.* **1950**, *18*, 1417.
(45) Cole, R. H.; Cole, K. S. *J. Chem. Phys.* **1942**, *10*, 98.
(46) Gregory, R. B.; Chai, K. J. *J. Phys. IV* **1993**, *3*, 305.
(47) Pissis, P. *J. Mol. Liq.* **1989**, *41*, 271.
(48) Pissis, P.; Anagnostopoulou-Konsta, A.; Apekis, L.; Daoukaki-Diamanti, D.; Christodoulides, C. *IEEE Trans. Electric. Insul.* **1992**, *27*, 820.
(49) Samouillan, V.; Lamure, A.; Lacabanne, C. *Chem. Phys.* **2000**, *255*, 259.
(50) Ibanoglu, E. *Food Chem.* **2005**, *90*, 621.
(51) Kremer, F.; Huwe, A.; Arndt, M.; Behrens, P.; Schwieger, W. *J. Phys.: Condens. Matter* **1999**, *11*, 175.
(52) Moznine, R. E.; Smith, G.; Polygalov, E.; Suherman, P. M.; Broadhead, J. *J. Phys. D: Appl. Phys.* **2003**, *36*, 330.
(53) Namikawa, H. *J. Non-Cryst. Solids* **1975**, *18*, 173.
(54) Dyre, J. C.; Schroder, T. B. *Rev. Mod. Phys.* **2000**, *72*, 873.
(55) Caliskan, G.; Mechtani, D.; Roh, J. H.; Kisliuk, A.; Sokolov, A. P.; Azzam, S.; Peral, I. *J. Chem. Phys.* **2004**, *121*, 1978.
(56) Sun, M.; Pejanovic, S.; Mijovic, J. M. *Macromolecules* **2005**, *38*, 9854.
(57) Mijovic, J.; Zhang, H. *Macromolecules* **2003**, *36*, 1279.

MA051854C